

Reevaluation of the Prospect of Observing Neutrinos from Galactic Sources in the Light of Recent Results in Gamma Ray and Neutrino Astronomy

M. C. Gonzalez-Garcia^{a,b,c} F. Halzen^d V. Niro^b

^a*Institució Catalana de Recerca i Estudis Avançats (ICREA)*

^b *Departament d'Estructura i Constituents de la Matèria and Institut de Ciències del Cosmos,
Universitat de Barcelona, Diagonal 647, E-08028 Barcelona, Spain*

^c *C.N. Yang Institute for Theoretical Physics, and Department of Physics and Astronomy, Stony Brook University,
Stony Brook, NY 11794-3840, USA*

^d *Wisconsin IceCube Particle Astrophysics Center and Department of Physics,
University of Wisconsin, Madison, WI 53706, USA*

Abstract

In light of the recent IceCube evidence for a flux of extraterrestrial neutrinos, we revisit the prospect of observing the sources of the Galactic cosmic rays. In particular, we update the predictions for the neutrino flux expected from sources in the nearby star-forming region in Cygnus taking into account recent TeV gamma ray measurements of their spectra. We consider the three Milagro sources: MGRO J2019+37, MGRO J1908+06 and MGRO J2031+41 and calculate the attainable confidence level limits and statistical significance as a function of the exposure time. We also evaluate the prospects for a kilometer-scale detector in the Mediterranean to observe and elucidate the origin of the cosmic neutrino flux measured by IceCube.

Email addresses: concha@insti.physics.sunysb.edu
(M. C. Gonzalez-Garcia), halzen@icecube.wisc.edu (F. Halzen),
niro@ecm.ub.edu (V. Niro).

1 Introduction

If supernova remnants are indeed the sources of the highest energy Galactic cosmic rays [1], the IceCube neutrino detector is expected to detect a flux of neutrinos accompanying the observed cosmic ray flux. Fermi has recently established the presence of pions in two supernova remnants thus unambiguously indicating the acceleration of cosmic rays [2]. However, their energies do not reach the PeV range and therefore the “PeVatrons” that are the sources of the cosmic rays in the “knee” region of the spectrum, and above, remain unidentified. Generic PeVatrons produce pionic gamma rays whose spectrum extends to several hundred TeV without a cutoff. Their predicted flux should be within reach of the present generation of ground-based gamma ray telescopes but has not been identified so far.

The highest energy survey of the Galactic plane to date has been performed by the Milagro detector. In particular, the survey in the 10 TeV band has revealed a subset of sources located within nearby star-forming regions in Cygnus and in the vicinity of Galactic latitude $l = 40$ degrees. Subsequently, directional air Cherenkov telescopes were pointed at some of the sources [3,4], revealing them as PeVatron candidates with gamma-ray fluxes following an E^{-2} energy spectrum that extends to tens of TeV without evidence for a cutoff. Interestingly, some of the sources cannot be readily associated with known supernova remnants, or with any non-thermal sources observed at other wavelengths. These are likely to be molecular clouds illuminated by the cosmic-ray beam accelerated in young remnants located within about 100 pc. Indeed one expects that multi-PeV cosmic rays are accelerated only over a short time period when the shock velocity is high, i.e., between free expansion and the beginning of its dissipation in the interstellar medium. The high-energy particles can produce photons and neutrinos over much longer periods when they diffuse through the interstellar medium to interact with nearby molecular clouds [5]. An association of molecular clouds and supernova remnants is expected in star-forming regions. Note that any confusion between pionic with synchrotron photons is unlikely to be a problem in this case.

Assuming that the Milagro sources are indeed cosmic-ray accelerators, the equality of the production of pions of all three charges dictates the relation between pionic gamma rays and neutrinos and basically predicts the production of a $\nu_\mu + \bar{\nu}_\mu$ pair for every two gamma rays seen by Milagro. The calculation can be performed in more detail with approximately the same outcome [6,7]. For average values of the source parameters it was anticipated that the completed IceCube detector should confirm sources in the Milagro sky map as sites of cosmic-ray acceleration at the 3σ level in less than one year and at the 5σ level in three years. This assumes that the source extends to 300 TeV, i.e. approximately 10% of the energy of the cosmic rays near the knee in the

spectrum. There are intrinsic ambiguities of an astrophysical nature in this estimate that may reduce or extend the time required for a 5σ observation [7], most prominently the exact location where the sources run out of energy. Also, the extended nature of some of the Milagro sources represents a challenge for IceCube observations that are optimized for point sources.

IceCube searches have revealed positive fluctuations from these sources in the 8 years of AMANDA data and in 4 out of 5 years of data collected with the partially deployed IceCube detector. On the other hand, the first extraterrestrial neutrino flux observed [8] by IceCube consists of 28 events (more below) with no event originating from the nearby star-forming region in Cygnus. This fact, together with the availability of new information from gamma ray telescopes, has motivated us to revisit the calculation of the neutrino flux in Ref. [7] for some of the sources. In particular we will update the information on MGRO J2019+37, MGRO J1908+06 and MGRO J2031+41 [9,10], 3 of the 6 sources used in the IceCube stacking analysis based on references [7,6,11].

As mentioned above, recently, IceCube has presented the first evidence for an extraterrestrial flux of very high-energy neutrinos, some with PeV energies. IceCube has thus become the latest entry in an extensive and diverse collection of instruments attempting to pinpoint the still enigmatic sources of cosmic rays. Analyzing data collected between May 2010 and May 2012, 28 neutrino events were identified with in-detector deposited energies between 30 and 1200 TeV. Among the 28 events, 21 are showers whose energies are measured to better than 15% but whose directions are determined to 10 – 15 degrees only. None show evidence for a muon track accompanying the neutrino. If of atmospheric origin, the neutrinos should be accompanied by muons produced in the air shower in which they originate. For example, the probability that a PeV atmospheric neutrino interacting in IceCube is unaccompanied by a muon is of order 0.1%. The remaining seven events are muon tracks. With the present statistics, these are difficult to separate from the competing atmospheric background. Fitting the data to a superposition of an extraterrestrial neutrino flux on an atmospheric background yields a cosmic neutrino flux of

$$E_\nu^2 \frac{dN_\nu}{dE_\nu} = 3.6 \times 10^{-11} \text{ TeV cm}^{-2} \text{ s}^{-1} \text{ sr}^{-1} \quad (1)$$

Of those 28 events, a hot spot of 7 shower events is evident at RA=281 degrees and dec=23 degrees close to the Galactic center although its significance is only 8% according to the test statistic defined in the blind analysis of the IceCube data. On the other hand, the highest energy event does reconstruct to within 1 degree of the Galactic center and, assuming an isotropic distribution, only 0.7 events are expected in the area of the sky covered by the seven showers. We will speculate that PeVatrons producing cosmic rays in the $10^{15} - 10^{17}$ energy range are the origin of these neutrinos. It is not unreasonable to expect that

PeVatrons cluster in the direction of the Galactic center corresponding to the largest concentration of mass along the line of sight. The star-forming region near the Galactic center itself is likely to be distant to be observed individually. We will investigate the opportunities for a kilometer-scale detector in the Northern hemisphere to elucidate the origin of the IceCube flux by observing muon neutrinos which allow for sub-degree angular reconstruction.

In Sec. 2 we update the gamma ray spectra from the three Milagro sources: MGRO J2019+37, MGRO J1908+06 and MGRO J2031+41 and the calculation of the associated neutrino event rates in IceCube. In Sec. 3 we study the attainable confidence level limits and statistical significance which Icecube can set as a function of the exposure time considering different values of the source parameters. We also estimate the prospects for a kilometer-scale detector in the Mediterranean to observe and elucidate the origin of the cosmic neutrino flux measured by IceCube. We briefly summarize our conclusions in Sec. 4.

2 Point sources

2.1 Neutrino flux

We start by updating the information on 3 of the 6 MILAGRO sources considered in past IceCube analyses. The parameters in Table 1 refer to the parametrization reported in Refs. [9,10], where the γ -ray flux in the TeV energy range is parametrized in terms of a spectral slope α_γ , an energy $E_{cut,\gamma}$ where the accelerator cuts off, and a normalization k_γ as

$$\frac{dN_\gamma(E_\gamma)}{dE_\gamma} = k_\gamma \left(\frac{E_\gamma}{\text{TeV}} \right)^{-\alpha_\gamma} \exp \left(-\frac{E_\gamma}{E_{cut,\gamma}} \right), \quad (2)$$

for a power law with cut-off fit and with

$$k_\gamma \equiv \frac{K}{E_{\text{norm}}^{-\alpha_\gamma}}, \quad (3)$$

where E_{norm} is the energy in TeV at which the flux is normalized, *i.e.* for $E \equiv E_{\text{norm}}$, the value of the flux dN_γ/dE_γ would be equivalent to K , in the absence of an energy cut-off. For sources without a cut-off the parametrization used is the one in Eq. (2) simply setting $E_{cut,\gamma} \rightarrow \infty$.

The neutrino fluxes associated with pionic gamma rays emitted by a source is directly determined by particle physics; approximately one $\nu_\mu + \bar{\nu}_\mu$ pair should accompany every 2 gamma rays. The exact relation between the gamma ray and neutrino fluxes has been described in detail in Ref.[12,13]. Their starting

Source	K [TeV ⁻¹ cm ⁻² s ⁻¹]	$E_{norm,i}$ [TeV]	$\alpha_{\gamma,i}$	$E_{cut,\gamma,i}$ [TeV]
MGRO J2019+37	$7_{-2}^{+5} \times 10^{-14}$	10	$2.0_{-1.0}^{+0.5}$	29_{-16}^{+50}
MGRO J1908+06	$6.1_{-1.4}^{+1.4} \times 10^{-13}$	4	$2.54_{-0.36}^{+0.36}$	–
MGRO J2031+41 ^(a)	$2.1_{-0.6}^{+0.6} \times 10^{-14}$	10	$3.22_{-0.18}^{+0.23}$	–
MGRO J2031+41 ^(b)	$5_{-3}^{+157} \times 10^{-14}$	10	$2.7_{-3.3}^{+0.7}$	$21_{-18}^{+\infty}$

Table 1

Best-fit values for MGRO J2019+37, MGRO J1908+06 and MGRO J2031+41, as reported in Refs. [9,10]. For the MGRO J2031+41 source, we report the values for a power law fit (a) and a power law with cut-off fit (b).

point, however, is a parametrization of the gamma-ray flux slightly different from the one in Eq.(2), namely

$$\frac{dN_{\gamma}(E_{\gamma})}{dE_{\gamma}} = k_{\gamma} \left(\frac{E_{\gamma}}{\text{TeV}} \right)^{-\alpha_{\gamma}} \exp \left(-\sqrt{\frac{E_{\gamma}}{E_{cut,\gamma}}} \right). \quad (4)$$

Thus we first find for each source the values of K , α_{γ} and $E_{cut,\gamma}$ in Eq.(4) which reproduce the range of gamma-ray fluxes obtained with the parametrization used by the experimental collaborations (2) with their determined parameters given in Table 1. The results of this *translation* for MGRO J2019+37, MGRO J1908+06, MGRO J2031+41 are given in Table 2 and the corresponding fluxes are plotted in Fig. 1 compared to those reported in Refs. [9,10] with parametrization (2).

Next, following the approximate relations given in Ref.[12,13] we can write the corresponding neutrino flux at the Earth after oscillations as

$$\frac{dN_{\nu_{\mu}+\bar{\nu}_{\mu}}(E_{\nu})}{dE_{\nu}} = k_{\nu} \left(\frac{E_{\nu}}{\text{TeV}} \right)^{-\alpha_{\nu}} \exp \left(-\sqrt{\frac{E_{\nu}}{E_{cut,\nu}}} \right), \quad (5)$$

with

$$\begin{aligned} k_{\nu} &= (0.694 - 0.16\alpha_{\gamma})k_{\gamma}, \\ \alpha_{\nu} &= \alpha_{\gamma}, \\ E_{cut,\nu} &= 0.59E_{cut,\gamma}. \end{aligned} \quad (6)$$

We will use Eq. (5) and Eq. (6) for the calculation of the neutrino flux from the different sources and to quantitatively evaluate the response of Icecube. Following Ref. [7] we will simulate the detection at the level of the secondary muons. This allows us to use the direct measurement of the muon energy to better characterize the expected signal.

Source	K [TeV ⁻¹ cm ⁻² s ⁻¹]	E_{norm} [TeV]	$\alpha_{\gamma,i}$	$E_{cut,\gamma,i}$ [TeV]
MGRO J2019+37	7×10^{-14}	10	1.8, 2.0, 2.2	30, 100, 300
MGRO J1908+06	6.1×10^{-13}	4	1.9, 2.1, 2.3	30, 100, 300
MGRO J2031+41	2.1×10^{-14}	10	2.6, 2.8, 3.0	30, 100, 300

Table 2

Values of K , E_{norm} , $\alpha_{\gamma,i}$ and $E_{cut,\gamma,i}$ that we used in our analysis. We refer to Eq. (4) and Eq. (3) for the definition of the variables.

2.2 Events

The number of events detected by IceCube from a source at zenith angle θ_Z can be written as [21,7]

$$\begin{aligned}
N_{ev} = t \times N_T \int dE_\nu dE_\mu^0 dE_\mu^{fin} & \left[\frac{dN_\nu(E_\nu)}{dE_\nu} \times Att_\nu(E_\nu, \theta_Z) \times \frac{d\sigma_\nu(E_\nu, E_\mu^0)}{dE_\mu^0} \right. \\
& \left. + \frac{dN_{\bar{\nu}}(E_\nu)}{dE_\nu} \times Att_{\bar{\nu}}(E_\nu, \theta_Z) \times \frac{d\sigma_{\bar{\nu}}(E_\nu, E_\mu^0)}{dE_\mu^0} \right] \\
& \times RR(E_\mu^0, E_\mu^{fin}) \times A_\mu^{eff}(E_\mu^{fin}, \theta_Z), \tag{7}
\end{aligned}$$

where we have summed over neutrinos and antineutrinos contributions. The neutrinos from the astrophysical sources or the atmospheric background interact with a cross section $\frac{d\sigma_\nu(E_\nu, E_\mu^0)}{dE_\mu^0}$ to yield a secondary muon of energy E_μ^0 . For the differential deep inelastic cross section $d\sigma_\nu(E_\nu, E_\mu^0)/dE_\mu^0$, we use the full expression (without any average inelasticity approximation) obtained with the CT10 NNLO PDFs [22] with $\alpha_s = 0.118$. For $x \leq 10^{-5}$ the PDF's are extrapolated using the double-log-approximation [23] following Refs. [24,25,26]. The muon propagation is taken into account by $RR(E_\mu^0, E_\mu^{fin})$, that describes the probability of a muon produced with initial energy E_μ^0 arriving at the detector with energy E_μ^{fin} after taking into account energy losses due to ionization, bremsstrahlung, e^+e^- pair production and nuclear interactions [27]. N_T is the target density of the material surrounding the detector, while $Att_{\nu(\bar{\nu})}(E_\nu, \theta_Z)$ is a factor which accounts for the attenuation of the flux due to neutrino (antineutrino) propagation in the Earth:

$$Att_{\nu(\bar{\nu})}(E_\nu, \theta_Z) = \exp[-X(\theta_Z)(\sigma_{NC}(E) + \sigma_{CC}(E))], \tag{8}$$

where $X(\theta_Z)$ is the column density of the Earth assuming the matter density profile of the Preliminary Reference Earth Model [28]. Finally the detector performance is described by its effective area for detecting muons $A_\mu^{eff}(E_\mu^{fin}, \theta_Z)$ and the exposure time t . For the functional form of the effective area we use the one reported in Ref. [7].

Source	R.A. [hh mm ss]	Dec. [dd mm ss]	σ_{ext}
MGRO J2019+37	20 18 35.03	+36 50 00.0	0.75°
MGRO J1908+06	19 07 54	+06 16 07	0.34°
MGRO J2031+41	20 29 38.4	+41 11 24	1.10°

Table 3

Position of the sources in right ascension and declination and extensions of the sources [10,17].

We use the Honda flux [29] to calculate the background of atmospheric neutrinos at the zenith angle corresponding to the source. We extrapolate this flux to higher energies to match the one from Volkova [30], that is known to describe the AMANDA data in the energy range of interest here. At high energy, the contribution of prompt neutrinos from charm decay cannot be neglected. We consider in this paper the model of Thunman *et al* (TIG) [31]. We integrate the atmospheric background over a solid angle $\Omega = \pi(1.6\sigma)^2$ around the direction of the source. The angle σ combines the effects of the angular resolution of the detector and the size of the source. For the size of the sources σ_{ext} , we refer to Table 3, while the angular resolution of IceCube σ_{IC} at these high energies is around 0.5°. The angle σ is then given by $\sqrt{\sigma_{\text{ext}}^2 + \sigma_{\text{IC}}^2}$. Assuming gaussianity, roughly 72% of the flux of the source is contained within this angular bin [32]. We will bin the events in the measured muon energy E_{μ}^{fin} assuming an energy resolution of 15% in $\log(E_{\mu}^{\text{fin}})$ for $E_{\mu}^{\text{fin}} \geq 1$ TeV.

In Fig. 2, we report the number of events for the sources MGRO J2019+37, MGRO J1908+06, MGRO J2031+41 and for the respective atmospheric background as a function of the measured muon energy. As described in the following section, we will use these spectra for the calculation of the confidence level at which a source could be excluded in the event of no observation of any signal events, as well as the statistical significance at which a source could be detected in the event of a positive observation, depending on the specific values of α_{γ} and $E_{\text{cut},\gamma}$.

3 Results

3.1 Milagro sources

As mentioned before the first extraterrestrial neutrino flux observed [8] by IceCube consists of 28 events with no event originating from nearby the Milagro sources. If this continues to be the case in the following years of operation, IceCube will be able to impose a bound on the probability of these sources to

be galactic PeVatrons. We refer to this probability as the Confidence Level of exclusion of a given source. Conversely if this is not the case and neutrinos are observed from the source direction in the amount expected by the estimates presented in the previous section IceCube will be able to establish the source as a galactic PeVatron with some probability. We refer to this as the Statistical Significance of discovery. We quantify these two statistical tests for the three Milagro sources as a function of the detector exposure and for a range of values of the source parameters α_γ and $E_{cut,\gamma}$ as we describe next.

To estimate the Confidence Level of exclusion of a given source we use as observable the total number of events with $E_\mu^{fin} \geq 1$ TeV without binning in energy. Generically, for the small statistics expected, the use of the total number of events yields a better rejection power than the use of the energy spectrum. We also studied the dependence of the Confidence Level of exclusion on the minimum E_μ^{fin} and found that as long as E_μ^{fin} was not so large that the number of expected background events became very small the Confidence Level of exclusion (C.L. from now on) did not change much.

Following standard techniques [33,34,35,36], we define C.L. as

$$C.L. = \frac{P_{(s+b)}}{1 - P_b}. \quad (9)$$

where $P_{(s+b)}$ and P_b are the p-values for the signal plus background and background only hypothesis of the data. Note that the denominator is present to avoid penalizing models to which one has little or no sensitivity. If $C.L. \leq \alpha$, a specific source is excluded with $(1 - \alpha)$ confidence level.

To obtain $P_{(s+b)}$ and P_b we first generate a large sample of event numbers that are Poisson distributed around the total expected number of background events and estimate what one could expect the “data” of IceCube to be in the absence of any signal, \mathcal{N}_D , as their median. Knowing the theoretical expectations, for signal plus background, $\mathcal{Y}_{(b+s)}$, and background only, \mathcal{Y}_b , we construct the data likelihood for signal plus background, $\mathcal{L}_{(s+b),D}$, and background only, $\mathcal{L}_{b,D}$.

We then generate a large number of experimental results N_{exp} , that are Poisson distributed around the expected total number of signal plus background (background only) events for which we can compute the corresponding likelihoods of signal+background $\mathcal{L}_{(s+b),J}$ (background only, $\mathcal{L}_{b,J}$) with $J = 1 \dots N_{exp}$ and count the number of results, $N_{pos}(s+b)$ ($N_{pos}(b)$) for which $-2 \ln \mathcal{L}_{(s+b),J} > -2 \ln \mathcal{L}_{(s+b),D}$ ($-2 \ln \mathcal{L}_{b,J} > -2 \ln \mathcal{L}_{b,D}$) so

$$P_{s+b} = \frac{N_{pos}(s+b)}{N_{exp}}, \quad 1 - P_b = \frac{N_{pos}(b)}{N_{exp}}. \quad (10)$$

The results for the expected C.L. are presented in Fig. 3 for the three sources considered in the paper and for the different values of α_γ and $E_{cut,\gamma}$, as reported in Table 2. From the figure we read for example that MGRO J2019+37, with $\alpha_\gamma = 1.8$ and $E_{cut,\gamma} = 300$ TeV, an exclusion at 99.9% (95%) is possible in 9 (4) years. Increasing the value of α_γ the exclusion limits get weaker as expected. For example, the values $\alpha_\gamma = 2.0$ and $E_{cut,\gamma} = 300$ TeV could be excluded at 95% confidence level in roughly 5 years, while $\alpha_\gamma = 2.2$ and $E_{cut,\gamma} = 300$ TeV in 8 years. For MGRO J1908+06, in 5 (2) years the values $\alpha_\gamma = 1.9$ and $E_{cut,\gamma} = 300$ TeV could be excluded at 99.9% (95%). Considering $\alpha_\gamma = 2.1$ and $E_{cut,\gamma} = 300$ TeV, an exclusion at 95% confidence level is possible in 4 years, while for, $\alpha_\gamma = 2.3$ and $E_{cut,\gamma} = 300$ TeV, 9 years are necessary for an exclusion at 95% confidence level. Finally for MGRO J2031+41, none of the parameters that we considered could be excluded at 95% confidence level in less than 10 years.

Conversely when estimating the Statistical Significance of discovery we find higher sensitivity to the signal when using the full spectral information of expected signal and background events. We compute the statistical significance of observing a signal as the background-only p-value, considering the analytic expression reported in Ref. [35]:

$$p_{\text{value}} = \frac{1}{2} \left[1 - \text{erf} \left(\sqrt{q_0^{\text{obs}}/2} \right) \right], \quad (11)$$

where q_0^{obs} is defined as

$$q_0^{\text{obs}} \equiv -2 \ln \mathcal{L}_{b,D} = 2 \sum_i \left(Y_{b,i} - N_{D,i} + N_{D,i} \ln \left(\frac{N_{D,i}}{Y_{b,i}} \right) \right), \quad (12)$$

with i running over the different energy bins. In this case $N_{D,i}$ is the estimated experimental data in bin i –generated as the median of a large sample of event numbers that are Poisson distributed around the expectation of signal plus background–, $Y_{b,i}$ is the theoretical expectation for the background hypothesis.

The results for the statistical significance are reported in Fig. 4. From the figure we read, for example that if the values of α_γ and $E_{cut,\gamma}$ for MGRO J2019+37 are equal to 1.8 and 300 TeV, respectively, the source could be detected at 5σ (3σ) in 9 (4) years. Increasing the value of α_γ , the statistical significances get weaker and, for example, the values $\alpha_\gamma = 2.0$ and $E_{cut,\gamma} = 300$ TeV could be excluded at 3σ in roughly 7 years, while $\alpha_\gamma = 2.2$, independently of the value of $E_{cut,\gamma}$, cannot be discovered at 3σ in less than 10 years. The second source that we considered, MGRO J1908+06, could be discovered at 5σ (3σ) in 6 (3) years if $\alpha_\gamma = 1.9$ and $E_{cut,\gamma} = 300$ TeV. Considering $\alpha_\gamma = 2.1$ and $E_{cut,\gamma} = 300$ TeV, a discovery at 3σ is possible in 6 years, while for $\alpha_\gamma = 2.3$, independently of the value of $E_{cut,\gamma}$, a discovery at 3σ is not possible in less than 10 years. Finally for the source MGRO J2031+41, none of the parameters

that we considered could lead to a discovery at 3σ in less than 10 years.

3.2 *IceCube evidence for cosmic neutrinos: are (some of) the neutrinos of Galactic origin?*

If cosmic accelerators are the origin of the extraterrestrial flux of neutrinos recently observed by IceCube [8], then the neutrinos have most likely been produced in proton-photon or proton-proton interactions with radiation or gas, either at the acceleration site or along the path traveled by cosmic rays to Earth. The fraction of energy transferred to pions is about 20% (50%) for $p\gamma$ (pp), respectively, and each of the three neutrinos from the decay chain $\pi^+ \rightarrow \mu^+\nu_\mu$ and $\mu^+ \rightarrow e^+\nu_e\bar{\nu}_\mu$ carries on average one quarter of the pion energy. Hence, the cosmic rays producing the excess neutrinos have energies of tens of PeV, well above the knee in the spectrum. It is tantalizingly close to the energy of 100 PeV [37,38] where the spectrum displays a rich structure, sometimes referred to as the ‘‘iron knee.’’ While these cosmic rays are commonly categorized as Galactic, with the transition to the extragalactic population at the ankle in the spectrum at $3 \sim 4$ EeV, one cannot rule out a subdominant contribution of PeV neutrinos of extragalactic origin. IceCube neutrinos may give us information on the much-debated transition energy.

The acceptance of the starting event analysis producing the first evidence for an extraterrestrial neutrino flux is such that the signal consist mostly of electron and tau neutrinos originating in the Southern hemisphere. While their energy can be reconstructed to 15%, their direction is only measured to $10 \sim 15$ degrees. In contrast, a detector in the Mediterranean views the Southern hemisphere through the Earth and therefore has sensitivity to muon neutrinos that can be reconstructed with sub-degree precision. For illustration, an IceCube detector cloned and positioned in the Mediterranean would observe a diffuse flux of 71 muon-neutrinos per year with energy in excess of 45 TeV for muon neutrino flux of:

$$E_\nu^2 \frac{dN_{\nu_\mu+\bar{\nu}_\mu}}{dE_\nu} = 1.2 \times 10^{-11} \text{ TeV cm}^{-2} \text{ s}^{-1} \text{ sr}^{-1}. \quad (13)$$

We here assumed a 1:1:1 distribution of flavors which is consistent with observation. Above 45 TeV, signal should be signal dominated providing a sky map with little background.

As mentioned in the introduction a cluster of seven events is observed close to the center of the Galaxy. If these events are originated from a point source, the corresponding flux would be

$$E_\nu^2 \frac{dN_{\nu_\mu+\bar{\nu}_\mu}}{dE_\nu} = 6 \times 10^{-11} \text{ TeV cm}^{-2} \text{ s}^{-1}, \quad (14)$$

corresponding to roughly 41 events per year, see Fig. 5 above 45 TeV in neutrino energy. This flux is simply estimated by multiplying the diffuse flux in Eq.(13) by $4\pi \times 7/17.4$ where we correct for the fact that 7 events out of 17.4 (we subtract the 10.6 of background estimation to the measured 28 events) are clustered around the Galactic Center and that both samples consist mainly of shower events.

Both the diffuse and point source signals would be statistically significant within one year. The operating Antares detector is a factor of 40 smaller than the IceCube detector, and therefore the IceCube excess only produces signals at the one-event level per year. Larger event samples, especially of well-reconstructed muon neutrinos, are likely to be the key to a conclusive identification of the origin of the IceCube extraterrestrial flux. If the flux observed in IceCube turns out to be isotropic, IceCube itself will observe the same muon neutrino signals from the Northern hemisphere.

If, on the other hand, any of the IceCube events do originate from a Galactic point source, IceCube itself should be able to observe the accompanying PeV gamma rays. The distance to the center of the Galaxy corresponds to a single interaction length for a PeV photon propagating in the microwave background. PeV photons are detected as muon-poor showers triggered by IceTop leaving no muons in IceCube. The level of point-source flux per neutrino flavor corresponding to one out of the 28 events is given by

$$E_\nu^2 \frac{dN_\nu}{dE_\nu} = 4\pi \frac{1}{28} 1.2 \times 10^{-11} \text{ cm}^{-2} \text{ s}^{-1} \text{ TeV} \\ \simeq 5.4 \times 10^{-12} \text{ cm}^{-2} \text{ s}^{-1} \text{ TeV}, \quad (15)$$

with the corresponding pionic photon flux a factor of 2 larger, assuming pp interactions; see above. This is a flux of $\sim 10^{-17} \text{ cm}^{-2} \text{ s}^{-1} \text{ TeV}^{-1}$ at 1 PeV, well within the gamma-ray sensitivity of the completed IceCube detector; see Fig. 15 in [39]. In fact, the highest fluctuation in a gamma-ray map obtained with one year of data collected with the detector when it was half complete is in the direction of one of the PeV neutrino events [40].

4 Summary

Recently, the IceCube detector reported evidence for extraterrestrial neutrinos, at very high-energies. Among the data collected between May 2010 and May 2012, 28 neutrino events were detected with energies between 20 and 1200 TeV, while from a background estimation roughly 10.6 events were expected. None of these events seems to originate from the nearby star-forming region

in Cygnus, posing the question of whether the observed gamma-ray sources in this region are indeed the postulated PeVatrons originating the galactic cosmic rays.

In view of these results and taking into account recent TeV gamma ray measurements of the spectra of some of the sources, we have updated the calculation of the neutrino expected from Milagro sources MGRO J2019+37, MGRO J1908+06 and MGRO J2031+41 3 of the 6 sources used in the IceCube stacking analysis based on references [7,6,11]. We have then estimated the confidence level with which IceCube could rule out these sources as galactic PeVatrons, should the results continue being negative in the following years of operation, or the statistical significance with which it can discover neutrinos from these sources if they are indeed galactic PeVatrons.

Moreover, among the 28 events, a hot spot of 7 shower events is evident at a position close to the Galactic Center. We studied the possibility of detecting the point-source flux associated to this hot spot by a kilometer-scale detector in the Northern hemisphere and by the Antares detector.

Acknowledgments

This work is supported by USA-NSF grant PHY-09-6739, by CUR Generalitat de Catalunya grant 2009SGR502 by MICINN FPA2010-20807 and consolidating program grants CUP (CSD-2008-00037) and CPAN, and by EU grant FP7 ITN INVISIBLES (Marie Curie Actions PITN-GA-2011-289442). F.H. is supported in part by the U.S. National Science Foundation under Grants No. OPP-0236449 and PHY-0969061 and by the University of Wisconsin Research Committee with funds granted by the Wisconsin Alumni Research Foundation.

References

- [1] W. Baade, F. Zwicky, On super-novae, Proceedings of the National Academy of Science 20 (1934) 254–259.
- [2] M. Ackermann, et al., Detection of the Characteristic Pion-Decay Signature in Supernova Remnants, Science 339 (2013) 807. [arXiv:1302.3307](#).
- [3] A. Djannati-Atai, E. Ona-Wilhelmi, M. Renaud, S. Hoppe, H.E.S.S. Galactic Plane Survey unveils a Milagro Hotspot. [arXiv:0710.2418](#).
- [4] J. Albert, et al., MAGIC observations of the unidentified TeV gamma-ray source TeV J2032+4130, *Astrophys.J.* 675 (2008) L25–L28. [arXiv:0801.2391](#).

- [5] S. Gabici, F. A. Aharonian, Searching for galactic cosmic ray pevatrons with multi-TeV gamma rays and neutrinos. [arXiv:0705.3011](#).
- [6] F. Halzen, A. Kappes, A. O’Murchadha, Prospects for identifying the sources of the Galactic cosmic rays with IceCube, *Phys.Rev.* D78 (2008) 063004. [arXiv:0803.0314](#).
- [7] M. Gonzalez-Garcia, F. Halzen, S. Mohapatra, Identifying Galactic PeVatrons with Neutrinos, *Astropart.Phys.* 31 (2009) 437–444. [arXiv:0902.1176](#).
- [8] M. Aartsen, et al., Evidence for high-energy extraterrestrial neutrinos at the IceCube detector, Accepted by Science.
- [9] B. Bartoli, et al., Observation of the TeV gamma-ray source MGRO J1908+06 with ARGO-YBJ. [arXiv:1207.6280](#).
- [10] A. Abdo, U. Abeysekara, B. Allen, T. Aune, D. Berley, et al., Spectrum and Morphology of the Two Brightest Milagro Sources in the Cygnus Region: MGRO J2019+37 and MGRO J2031+41, *Astrophys.J.* 753 (2012) 159. [arXiv:1202.0846](#).
- [11] A. Kappes, F. Halzen, A. O. Murchadha, Prospects of identifying the sources of the galactic cosmic rays with IceCube, *Nucl.Instrum.Meth.* A602 (2009) 117–119.
- [12] S. Kelner, F. A. Aharonian, V. Bugayov, Energy spectra of gamma-rays, electrons and neutrinos produced at proton-proton interactions in the very high energy regime, *Phys.Rev.* D74 (2006) 034018. [arXiv:astro-ph/0606058](#).
- [13] A. Kappes, J. Hinton, C. Stegmann, F. A. Aharonian, Potential Neutrino Signals from Galactic Gamma-Ray Sources, *Astrophys.J.* 656 (2007) 870–896. [arXiv:astro-ph/0607286](#).
- [14] A. Abdo, B. T. Allen, D. Berley, S. Casanova, C. Chen, et al., TeV Gamma-Ray Sources from a Survey of the Galactic Plane with Milagro, *Astrophys.J.* 664 (2007) L91–L94. [arXiv:0705.0707](#).
- [15] A. Abdo, B. Allen, T. Aune, D. Berley, C. Chen, et al., Milagro Observations of TeV Emission from Galactic Sources in the Fermi Bright Source List, *Astrophys.J.* 700 (2009) L127–L131. [arXiv:0904.1018](#).
- [16] B. Bartoli, P. Bernardini, X. Bi, C. Bleve, I. Bolognino, et al., Observation of TeV gamma rays from the Cygnus region with the ARGO-YBJ experiment, *Astrophys.J.* 745 (2012) L22. [arXiv:1201.1973](#).
- [17] F. Aharonian, Detection of Very High Energy radiation from HESS J1908+063 confirms the Milagro unidentified source MGRO J1908+06. [arXiv:0904.3409](#).
- [18] A. J. Smith, A Survey of Fermi Catalog Sources using Data from the Milagro Gamma-Ray Observatory. [arXiv:1001.3695](#).
- [19] F. Aharonian, et al., The Unidentified TeV source (TeV J2032+4130) and surrounding field: Final HEGRA IACT-system results, *Astron.Astrophys.* 431 (2005) 197–202. [arXiv:astro-ph/0501667](#).

- [20] M. J. Lang, D. Carter-Lewis, D. Fegan, S. Fegan, A. Hillas, et al., Evidence for TeV gamma ray emission from TeV j2032+4130 in whipple archival data, *Astron.Astrophys.* 423 (2004) 415–419. [arXiv:astro-ph/0405513](#).
- [21] M. Gonzalez-Garcia, F. Halzen, M. Maltoni, Physics reach of high-energy and high-statistics icecube atmospheric neutrino data, *Phys.Rev.* D71 (2005) 093010. [arXiv:hep-ph/0502223](#).
- [22] J. Gao, M. Guzzi, J. Huston, H.-L. Lai, Z. Li, et al., The CT10 NNLO Global Analysis of QCD. [arXiv:1302.6246](#).
- [23] L. Gribov, E. Levin, M. Ryskin, Semihard Processes in QCD, *Phys.Rept.* 100 (1983) 1–150.
- [24] C. Quigg, M. Reno, T. Walker, Interactions of Ultrahigh-Energy Neutrinos, *Phys.Rev.Lett.* 57 (1986) 774.
- [25] M. Reno, C. Quigg, On the Detection of Ultrahigh-Energy Neutrinos, *Phys.Rev.* D37 (1988) 657.
- [26] R. Gandhi, C. Quigg, M. H. Reno, I. Sarcevic, Ultrahigh-energy neutrino interactions, *Astropart.Phys.* 5 (1996) 81–110. [arXiv:hep-ph/9512364](#).
- [27] P. Lipari, T. Stanev, Propagation of multi - TeV muons, *Phys.Rev.* D44 (1991) 3543–3554.
- [28] A. Dziewonski, D. Anderson, Preliminary reference earth model, *Phys.Earth Planet.Interiors* 25 (1981) 297–356.
- [29] M. Honda, T. Kajita, K. Kasahara, S. Midorikawa, Improvement of low energy atmospheric neutrino flux calculation using the JAM nuclear interaction model, *Phys.Rev.* D83 (2011) 123001. [arXiv:1102.2688](#).
- [30] L. Volkova, Energy Spectra and Angular Distributions of Atmospheric Neutrinos, *Sov.J.Nucl.Phys.* 31 (1980) 784–790.
- [31] P. Gondolo, G. Ingelman, M. Thunman, Charm production and high-energy atmospheric muon and neutrino fluxes, *Astropart.Phys.* 5 (1996) 309–332. [arXiv:hep-ph/9505417](#).
- [32] D. Alexandreas, D. Berley, S. Biller, G. Dion, J. Goodman, et al., Point source search techniques in ultrahigh-energy gamma-ray astronomy, *Nucl.Instrum.Meth.* A328 (1993) 570–577.
- [33] T. Junk, Confidence level computation for combining searches with small statistics, *Nucl.Instrum.Meth.* A434 (1999) 435–443. [arXiv:hep-ex/9902006](#).
- [34] A. L. Read, Modified frequentist analysis of search results (The CL(s) method), CERN-OPEN-2000-205.
- [35] Procedure for the LHC Higgs boson search combination in summer 2011, ATL-PHYS-PUB-2011-011, ATL-COM-PHYS-2011-818, CMS-NOTE-2011-005.
- [36] J. Beringer, et al., Review of Particle Physics, *Phys.Rev.* D86 (2012) 010001.

- [37] W. Apel, J. Arteaga, L. Bhren, K. Bekk, M. Bertaina, et al., Thunderstorm Observations by Air-Shower Radio Antenna Arrays. [arXiv:1303.7068](#).
- [38] M. Aartsen, et al., Measurement of the cosmic ray energy spectrum with IceTop-73. [arXiv:1307.3795](#).
- [39] M. Aartsen, et al., Search for Galactic PeV Gamma Rays with the IceCube Neutrino Observatory, *Phys.Rev. D*87 (2013) 062002. [arXiv:1210.7992](#).
- [40] M. Ahlers, K. Murase, Probing the Galactic Origin of the IceCube Excess with Gamma-Rays. [arXiv:1309.4077](#).

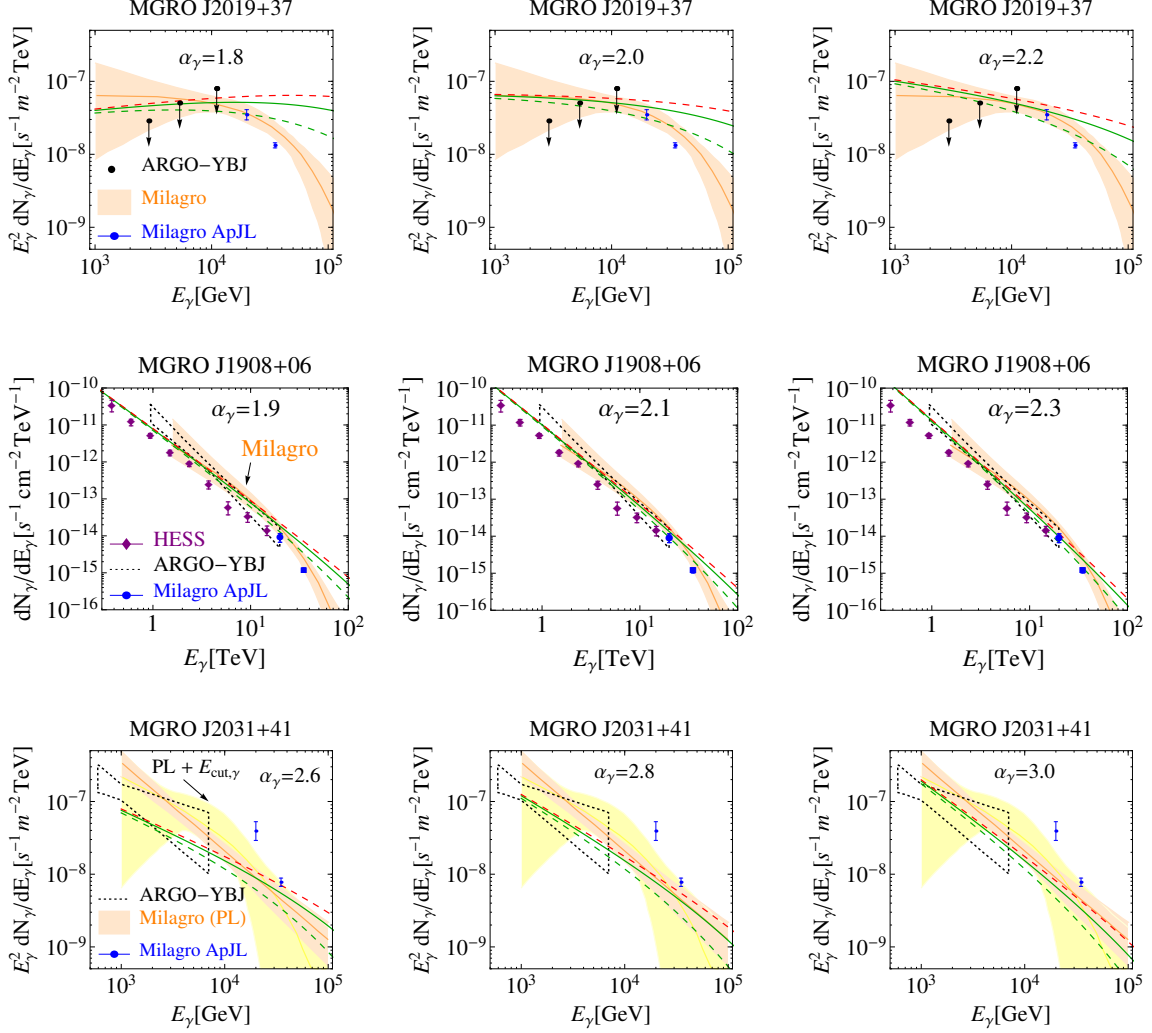


Fig. 1. Flux of γ -rays using our parametrization of Eq. (4). The source flux has been normalized to the values of K reported in Table 2. The green dashed, solid green and red dashed lines refer to $E_{cut,\gamma} = 30, 100, 300$ TeV, respectively. For MGRO J2019+37, the continuous orange line is the best fit to the Milagro data, while the shaded orange area represents the 1σ band [10]. With blue lines, we report also the previous flux measurements by Milagro at 20 TeV and 35 TeV [14,15]. The 90% CL upper limits from ARGO-YBJ are shown in black [16]. For MGRO J1908+06, we show in purple the data by HESS [17] and in blue the previous flux measurements by Milagro [14,15]. The dotted area shows the ARGO-YBJ 1σ band [9], while the solid orange line and the shaded orange area show the best fit and the 1σ band by Milagro [18]. For MGRO J2031+41, the power law model is shown in orange and the power law model with cut-off is shown in yellow [10]. The previous flux measurements by Milagro are shown in blue [14,15]. With dotted lines, we report the spectrum measured by ARGO-YBJ [16]. Note that for MGRO J2031+41, we didn't report the measurements by MAGIC [4] and HEGRA [19]. These measurements are mutually consistent, but they disagree with the best fit and 1σ region obtained by Milagro [10], considering both a power-law and a power-law with energy cut-off. In addition, the flux at 0.6 TeV was measured also by Whipple, see Ref. [20] for more details.

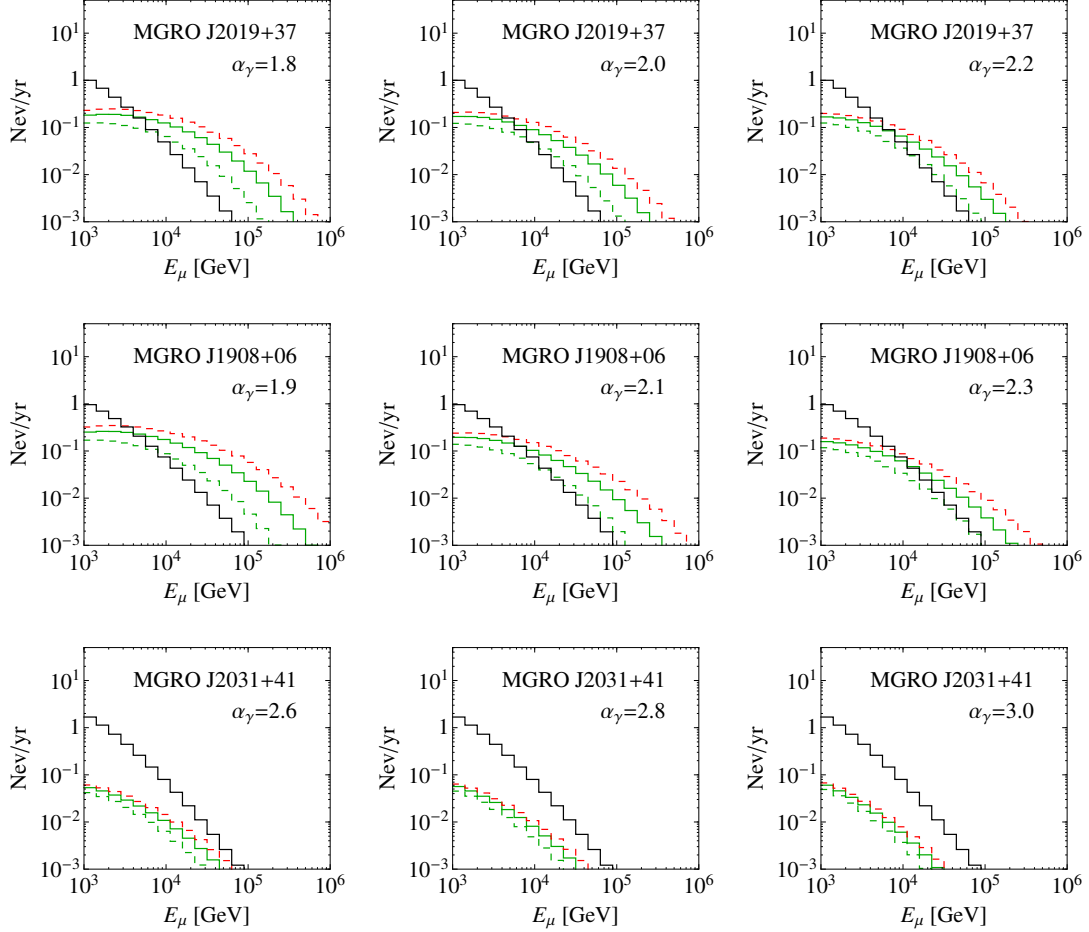


Fig. 2. Number of events for the three Milagro sources with different values of α_γ and $E_{cut,\gamma} = 30, 100, 300$ TeV for green dashed, solid green and red dashed, respectively. The source fluxes have been normalized as reported in Table 2. The black lines represent the atmospheric neutrino background, integrated over a solid angle equal to $\Omega = \pi(1.6 \sigma)^2$, with $\sigma = 0.9^\circ$ for MGRO J2019+37 and 0.6° for MGRO J1908+06 and 1.2° for MGRO J2031+41. A correction for the size of the source has been introduced (factor 72%).

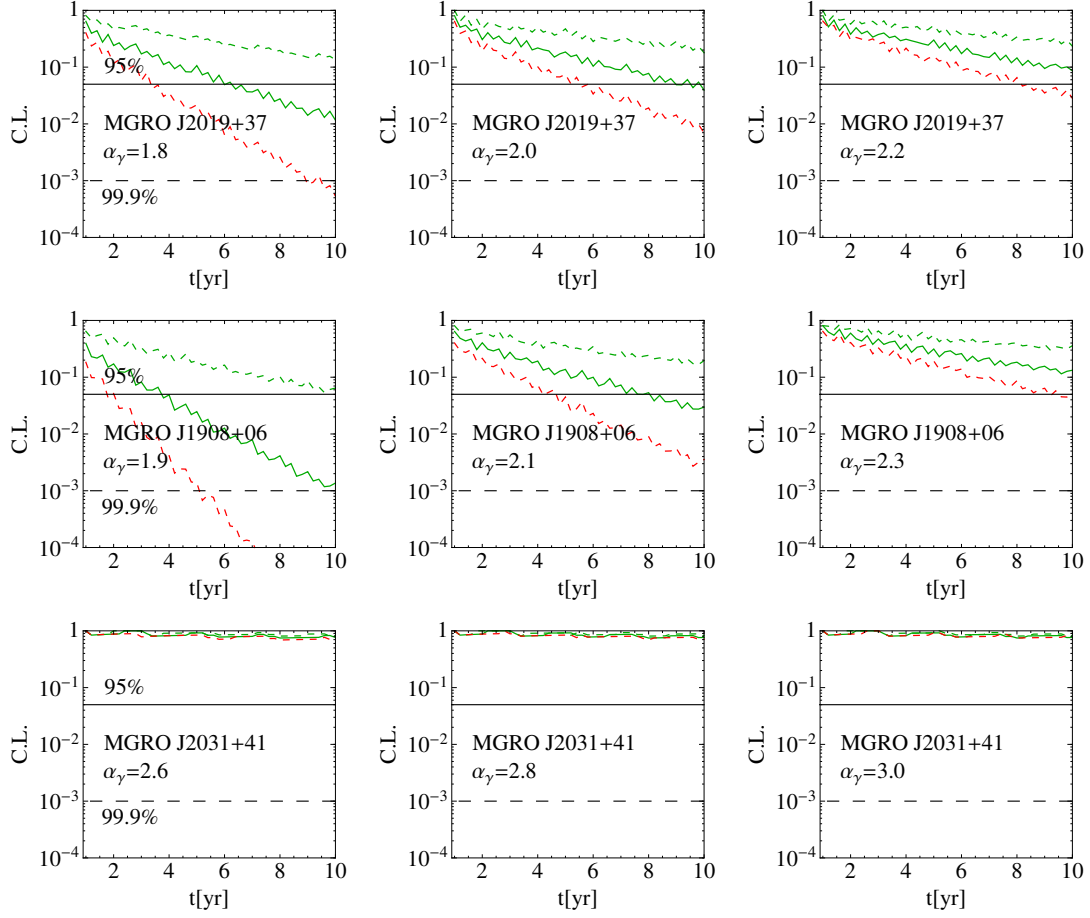


Fig. 3. Confidence level at which a source could be excluded as a function of time. For each sources, we have considered different values of α_γ and $E_{cut,\gamma} = 30, 100, 300$ TeV for green dashed, solid green and red dashed, respectively. The observed spectra are obtained as the median of random generated values around the background.

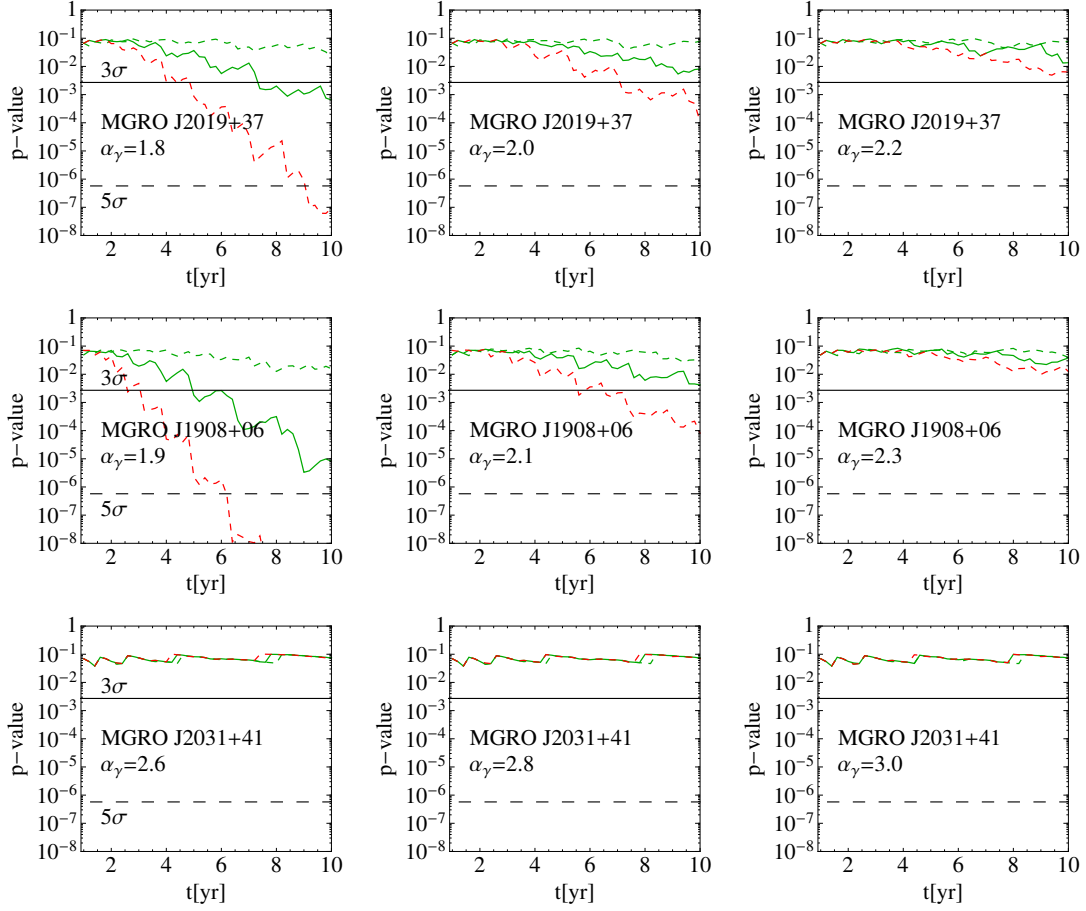


Fig. 4. Statistical significance at which a source could be detected as a function of time. For each source, we considered different values of α_γ and $E_{cut,\gamma} = 30, 100, 300$ TeV for green dashed, solid green and red dashed, respectively. The observed spectra are obtained as the median of random generated values around the signal plus background.

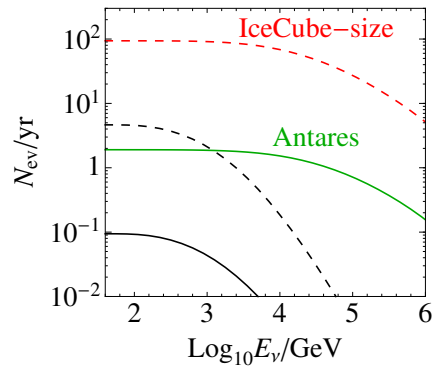


Fig. 5. Events from Galactic Center source as a function of the neutrino energy. We report the number of events and the background for an IceCube-size detector in the north hemisphere (red-dashed line) and for Antares (green-solid line), together with the respective atmospheric background: black-dashed for IceCube and black-solid for Antares. For the atmospheric background we have integrated over a steradian $\Omega = \pi(1.6\sigma)^2$, with $\sigma = 0.4^\circ$.